ELECTROWEAK SYMMETRY BREAKING WITHOUT A HIGGS BOSON AT THE LHC

Sarah Allwood-Spiers
On behalf of the ATLAS and CMS Collaborations
University of Glasgow, Glasgow G12 8QQ, UK.

We present two studies into strong symmetry breaking scenarios at the LHC. The first case is a study into vector boson scattering at ATLAS. This uses the framework of the Electroweak Chiral Lagrangian with Padé unitarisation to generate possible signal scenarios. Signals could be observed with an integrated luminosity of $\int \mathrm{Ldt} \simeq 30$ fb^{-1}. Secondly a search for the technirho, ρ_{TC}, at CMS is presented, within the Technicolour "Straw Man" model. 5σ discovery is possible starting from $\int \mathrm{Ldt} \simeq 4$ fb^{-1}.

1 Introduction

It is possible that the higgs boson does not exist, and that a weakly-coupled model is not responsible for electroweak symmetry breaking. An alternative is that electroweak symmetry breaking results from new strong interactions. Since the Goldstone bosons resulting from spontaneous symmetry breaking become the longitudinal components of the W and Z bosons at high energy, we can probe the electroweak symmetry breaking sector by studying vector boson interactions.

Strong electroweak symmetry breaking scenarios can be treated quite generally by an effective Lagrangian approach, using the Electroweak Chiral Lagrangian accompanied by some unitarity constraints. A study of vector boson scattering using this framework at ATLAS is presented in section 2. Under the more specific Technicolour "Straw Man" model, a search for the technirho, ρ_{TC}, at CMS is presented in section 3.

2 Electroweak Chiral Lagrangian Studies at ATLAS

The Electroweak Chiral Lagrangian [1] (EWChL) describes electroweak interactions at energies less than 1 TeV. It is built as an expansion in the Goldstone boson momenta. If it is assumed that custodial symmetry is conserved, there are only two, dimension-4, terms that describe the quartic couplings of the longitudinal vector bosons

$$\mathcal{L}^{(4)} = a_4 (Tr(D_\mu U D^\nu U^\dagger))^2 + a_5 (Tr(D_\mu U D^\mu U^\dagger))^2 \quad (1)$$

where the Goldstone bosons ω_a (a=1,2,3) appear in the group element $U = e^{\left(i\frac{\vec{\omega}\cdot\vec{\sigma}}{v}\right)}$, σ are the Pauli matrices and $v = 246$ GeV. Hence the low-energy effect of the underlying physics in vector boson scattering is parameterised by the coefficients a_4 and a_5.

The Lagrangian does not respect unitarity. To extend its validity range to the higher energies that we will be probing at the LHC, a unitarisation procedure must be imposed, which can lead to

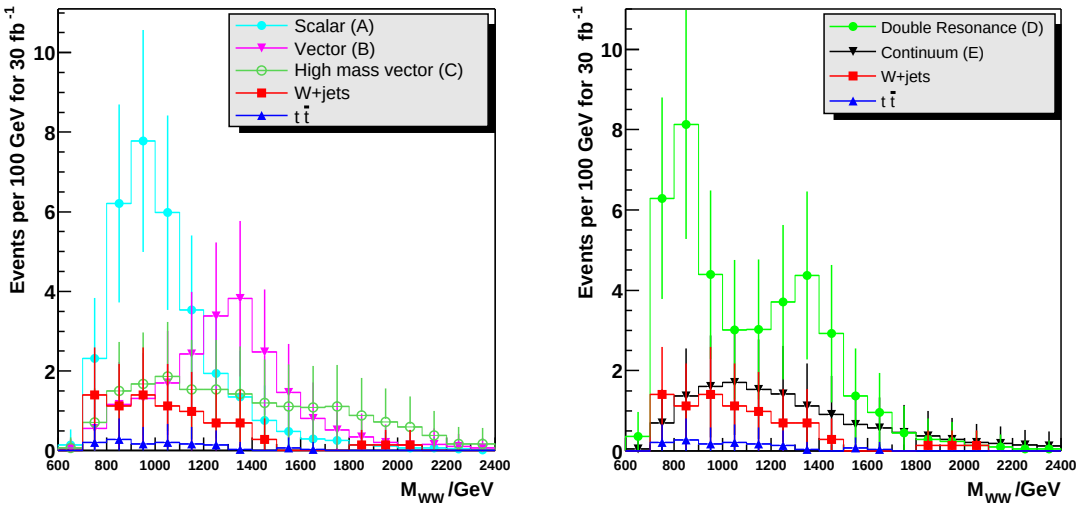

Figure 1: Reconstructed WW mass for 5 signal scenarios after all cuts.

resonances developing in $[a_4, a_5]$ space. This is dependent on the chosen unitarisation procedure; in the work presented here the Padé or Inverse Amplitude method was used [2].

There have been several studies of EWChL signals in vector boson scattering at ATLAS. All seek to exploit the distinctive characteristics of the vector boson fusion process. The boson-boson centre-of-mass energy of interest is ∼1 TeV, so the bosons have high-p_T. There are two high energy forward tag jets originating from the quarks that emitted the bosons. Since vector bosons are colourless, there is no colour connection between the tag quarks and hence no additional QCD radiation in the central region.

2.1 WW Scattering: $qqWW \rightarrow q'q'WW$

An analysis of $WW \rightarrow l\nu qq$ using the ATLAS fast simulation, ATLFAST, to simulate the effects of the detector is presented here [3,4]. Five signal points in $[a_4, a_5]$ space are chosen; after unitarisation these result in a scalar resonance with a mass of 1 TeV (A), a vector resonance of 1.4 TeV (B), a vector of 1.8 TeV (C), a double resonance of a scalar and a vector (D), and a continuum scenario (E). This final no-resonance scenario is the most pessimistic, with a cross-section×branching ratio of 13 fb. Pythia [5], modified to include the EWChL, is used to simulate the signal and the W+jets (where $W \rightarrow l\nu$) and $t\bar{t}$ backgrounds.

The leptonically-decaying W is reconstructed from the highest-p_T lepton and the missing transverse energy, E_T^{miss}. The lepton 4-momentum, E_T^{miss} and W mass constraint yield a quadratic equation for the z-component of neutrino momentum, p_Z^ν. The minimum p_Z^ν solution is chosen because it is closest to the true p_Z^ν in the majority of cases. A cut of $p_T > 320$ GeV is made on this W candidate.

The hadronically-decaying W is highly boosted and can be identified as one or two jets. When jets are identified using the k_T algorithm [6], the highest-p_T jet is chosen as the hadronic W candidate. It is required to have $p_T > 320$ GeV and a mass close to m_W. A further "subjet" cut is performed. The k_T algorithm is re-run in subjet mode over the constituents of this jet and the scale at which the jet is resolved into two subjets, $y_{21}p_T^2$, is found [7]. For a true W, this scale is close to m_W^2. A cut requiring $1.55 < \log(p_T\sqrt{y_{21}}) < 2.0$ reduces the W+jets background.

To reduce the $t\bar{t}$ background, a crude reconstruction of tops is performed by combining either W candidate with any other jet in the event. Events in which the invariant mass of any of these combinations is close to m_t are rejected. The two tag jets are identified as the highest-p_T jets forward and backward of the W candidates, and required to have $E > 300$ GeV and $|\eta| > 2$. The

p_T of the full system should be zero, so events with $p_T(WW + \text{tagjets}) > 50$ GeV are rejected. Finally, events containing more than one additional central jet with $p_T > 20$ GeV are rejected.

The reconstructed WW mass after all cuts is shown in figure 1 for the five chosen signal scenarios. All signals are observable above the W+jets and $t\bar{t}$ backgrounds with an integrated luminosity of $\int \text{Ldt} \simeq 30$ fb^{-1}, with the continuum signal achieving a significance of $s/\sqrt{b} = 4.7$.

2.2 WZ Scattering: $qqWZ \to q'q'WZ$

A 1.2 TeV vector resonance in WZ scattering with $WZ \to jjll$ (which has $\sigma \times BR = 2.8$ fb) was investigated using ATLFAST. The analysis considerations are similar to the above WW study. although a different implementation of cuts is chosen. After all analysis cuts the only significant background is from Z+jets production: for 100 fb^{-1}, 14 signal events and 3 background events are expected in the peak region [8]. The reconstructed WZ mass is shown in figure 2. A recent

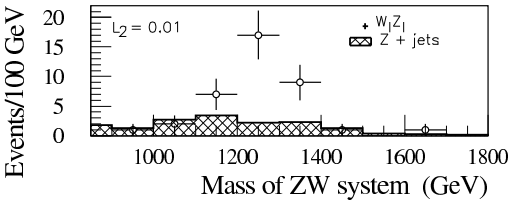

Figure 2: Reconstructed WZ mass for $WZ \to jjll$ after all cuts for 300 fb^{-1}.

study using the ATLAS full detector simulation verifies this result, and also finds that significant signals can be observed with 100 fb^{-1} in the $WZ \to l\nu qq$ mode and 300 fb^{-1} in the $WZ \to l\nu ll$ mode[9]. Updated WW and WZ scattering analyses will be presented in the forthcoming ATLAS "Computing System Commissioning" note to be completed in summer 2007.

3 Search for the technirho, ρ_{TC}, at CMS

The original model of Technicolour (TC) is a scaled-up version of QCD; a new set of interactions is introduced with the same physics as QCD, but at an energy scale $\Lambda_{TC} \sim 200$ GeV. The new strong interaction emerging at the electroweak scale is mediated by $N_{TC}^2 - 1$ technigluons. Electroweak symmetry breaking results from the formation of a technifermion condensate, producing Goldstone bosons (the technipions). Three of the technipions become the longitudinal components of the $W^{\pm}$ and Z bosons.

To generate fermion masses, "Extended Technicolour" interactions are introduced, and the technicolour gauge coupling is required to vary more slowly as a function of the renormalisation scale (it is a "walking" rather than a running coupling). The result is that many technifermions are predicted, and the lightest technicolour resonances appear below 1 TeV. Acquiring the correct top quark mass is a further complication; this is achieved by Topcolour-Assisted Technicolour.

The Technicolour "Straw Man" model sets the framework for searching for the lightest bound states. assuming that these can be considered in isolation [10]. Here we present a search for the colour-singlet ρ_{TC} in this framework using the CMS detector. The analysis [11] considers the channel $q\bar{q} \to \rho_{TC} \to WZ$ for 14 signal points in [$m(\rho_{TC})$,$m(\pi_{TC})$] space. The cleanest decay mode, $\rho_{TC} \to WZ \to l\nu ll$ is chosen. The $\sigma \times$ BR for these signals range from 1 fb to 370 fb.

The main backgrounds are from $WZ \to l\nu ll$ and $ZZ \to llll$, $Zb\bar{b} \to ll + X$ and $t\bar{t}$. All signals and backgrounds are generated using Pythia [5]. The CMS fast simulation FAMOS is used, with lepton reconstruction efficiencies and resolutions validated against the GEANT-based full detector simulation.

The three highest-p_T leptons (electrons or muons) in the event are selected. Making appropriate isolation cuts in the initial identification of these lepton candidates is important in

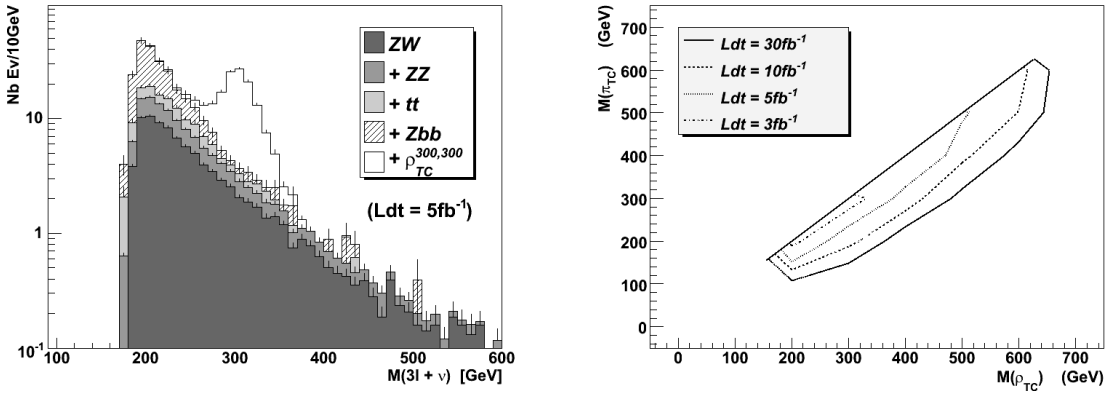

Figure 3: (left) Reconstructed ρ_{TC} mass after all cuts, (right) Sensitivity contours for 5σ discovery of ρ_{TC} at various integrated luminosities, assuming the default parameters of the TC Straw Man model.

reducing the $Zb\bar{b}$ and $t\bar{t}$ backgrounds. The Z is reconstructed from two same flavour opposite sign leptons. The W is reconstructed from the third lepton and E_T^{miss}, as explained in section 2.1.

Kinematic cuts on the W and Z candidates are needed to improve the signal to background ratio. The W and Z candidates are each required to have $p_T > 30$ GeV. A Z mass window cut of $|m_{l^+l^-} - m_Z| < 3\sigma$ is particularly effective in reducing the $t\bar{t}$ background. Finally, a cut on the pseudorapidity difference between the W and Z of $|\eta(Z) - \eta(W)| < 1.2$ is effective in reducing the WZ background, although this remains the largest background after all cuts as shown in figure 3(a).

The expected signal sensitivity is computed using the sum of the reconstructed ρ_{TC} mass spectra for the signal and backgrounds, taking into account the statistical fluctuations for a given integrated luminosity. It is assumed that the probability density function is Gaussian for the signal and exponential for the background. The sensitivity estimator is given by $S_{\mathcal{L}} = \sqrt{2\ln(\mathcal{L}_{\mathcal{S}+\mathcal{B}}/\mathcal{L}_{\mathcal{B}})}$, where $\mathcal{L}_{\mathcal{S}+\mathcal{B}}$, the signal plus background hypothesis, and $\mathcal{L}_{\mathcal{B}}$, the null hypothesis. The sensitivity is computed for each signal point and the resulting contour plot in $[m(p_{TC}), m(\pi_{TC})]$ space is shown in figure 3(a). 5σ sensitivities are obtained for integrated luminosities starting from 3 fb^{-1}, before accounting for systematic uncertainties. Including the expected systematic uncertainties due to the detector, 5σ discovery is possible starting from 4 fb^{-1} of data.

References

1. T. Appelquist, & C.W. Bernard, 1980, *Phys. Rev.* **D22** 200.
2. A. Dobado, M.J. Herrero, J.R. Pelaez, & E. Ruiz Morales, 2000, *Phys. Rev.* **D62**, 055011.
3. S. Allwood, 2006, University of Manchester, PhD Thesis.
4. E. Stefanidis, 2007, University College London, Ph.D. Thesis.
5. T. Sjostrand, L. Lonnblad, & S. Mrenna, 2001, [arXiv:hep-ph/0108264].
6. J.M. Butterworth, J.P. Couchman, B.E. Cox, & B.M. Waugh, 2003, *Comput. Phys. Commun.*, 153:85-96.
7. J.M. Butterworth, B.E. Cox, & J.R. Forshaw, 2002, *Phys. Rev.* **D65**, 096014.
8. A. Myagkov, 1999, ATL-PHYS-99-006.
9. G. Azuelos, P.A. Delsart, J. Idarraga, & A. Myagkov, 2006, ATL-COM-PHYS-2006-041.
10. K. Lane & S. Mrenna, 2003, *Phys. Rev.* **D67**, 115011.
11. P. Kreuzer, 2006, CERN-CMS-NOTE-2006-135.